Food Chemistry: X 35 (2026) 103782

Contents lists available at ScienceDirect

Food Chemistry: X

journal homepage: www.sciencedirect.com/journal/food-chemistry-x

An AuNP-labeled triple-helix molecular switch for ultrasensitive, on-site detection of tetracycline in milk via fiber-optic localized surface plasmon resonance biosensing

Xuqi Situ, Jiacong Li, Yeshun Zhang, Hui Yan *

School of biotechnology, Jiangsu University of Science and technology, Zhenjiang 212100, China

ARTICLE INFO

Keywords:
Localized surface plasmon resonance
fiber-optic biosensor
Triple-helix molecular switch
Tetracycline
Food safety

ABSTRACT

To meet the urgent demand for monitoring tetracycline residues in milk—a critical food for vulnerable groups a novel fiber-optic Localized Surface Plasmon Resonance (LSPR) biosensor was engineered using gold-nanoparticle-labeled DNA triple-helix switches. The sensor operates via a target-activated disassembly: tetracycline binding dissociates the immobilized triple-helix, releasing gold nanoparticles and inducing a measurable LSPR blue shift. This active displacement amplifies the signal via localized refractive-index changes, enabling rapid, label-free detection. The sensor achieved excellent performance, with a linear range of 5–100 ng/mL and a low detection limit of 0.28 ng/mL. When applied to real milk samples, it delivered excellent recovery rates of 96.75%–104.15% (RSD <5.1%) and showed no statistically significant difference ($p > 0.05$) compared to HPLC reference analysis. Combining high sensitivity with a modular, engineering-flexible design, this platform not only provides a practical solution for on-site tetracycline screening in food safety but also holds significant potential for adapting to other antibiotics and environmental targets, extending its utility beyond dairy monitoring.

1. Introduction

Since its discovery in the 1940s, tetracycline has gained extensive application in the global veterinary and livestock sectors due to its low cost and remarkable antibacterial efficacy(Pollard & Morra, 2018; Wang et al., 2024). As a broad-spectrum antibiotic, tetracycline is frequently employed as a prophylactic agent, incorporated in animal feed to control infections and enhance animal growth. However, the rapid expansion of the livestock industry has been accompanied by the irrational use of tetracycline. After ingestion by animals, tetracycline can accumulate in the human body through the food chain, potentially exerting toxic effects on organs such as the liver(Liu et al., 2019). Moreover; the improper use of tetracycline may also induce severe adverse reactions; such as esophageal perforation and pseudotumor cerebri (Angelette et al., 2023).The detrimental effects of tetracycline on humans are not confined to adults but also extend to the growth and development of fetuses. The drug can traverse the placental barrier; enter the fetal body; and accumulate in developing bones and teeth; particularly during the formation of enamel and dentin; leading to yellow discoloration of fetal teeth(Jia, Zhang, Zhu, & Xu, 2022; Madison, 1963).

Given that tetracycline can adversely affect human health even at low concentrations, the European Union (EU) and the U.S. Food and Drug Administration (FDA) have established stringent maximum residue limits (MRLs) for tetracycline in various animal-derived food products, with particular attention to milk: the EU sets the limit at 0.1 mg/kg, while the FDA allows up to 0.3 mg/kg. As a staple food with high daily consumption and frequent intake by infants and other vulnerable groups, milk's residue level is directly linked to the prevention and control of public health risks (Liu et al., 2018; Meng, Sun, Xing, & Dong, 2026; Wen et al., 2025). If detection is delayed or inaccurate, products exceeding the limit may enter the market and pose potential harm through long-term exposure. Therefore, establishing rapid and reliable detection methods suitable for high-risk foods such as milk has become an essential prerequisite for food safety regulation. Against this backdrop, developing detection technologies capable of on-site screening is of great importance for safeguarding milk quality and public health.

Effective mitigation and prevention of environmental and food contamination resulting from the misuse of tetracycline rely heavily on timely and accurate detection. Conventional analytical techniques for tetracycline monitoring include high-performance liquid chromatography (HPLC) (Tsuji & Goetz, 1978); enzyme-linked immunosorbent assay (ELISA) (Aga, Goldfish, & Kulshrestha, 2003); liquid

* Corresponding author at: Jiangsu University of Science and Technology, Zhenjiang 212100, China.
E-mail address: yan_hui@just.edu.cn (H. Yan).

https://doi.org/10.1016/j.fochx.2026.103782
Received 28 November 2025; Received in revised form 14 February 2026; Accepted 21 March 2026
Available online 27 March 2026

chromatography–tandem mass spectrometry (LC–MS/MS) (Gad, 2024); and microbiological assays (Druzhinina, 1961)]. Although these methods offer reliable quantification, they are often limited by complex sample preparation, high instrumentation costs, prolonged analysis times, and the inability to support on-site or real-time monitoring. In contrast, biosensor technology has emerged as a promising alternative that offers rapid detection, minimal instrumentation requirements, and the potential for real-time, on-site analysis, thereby overcoming key limitations of conventional approaches.

As a cornerstone of modern analytical science, biosensors have become indispensable in medical diagnostics, environmental monitoring, and food safety owing to their high sensitivity, selectivity, and real-time analytical capability. A biosensor typically integrates a biorecognition element, such as enzymes, antibodies, nucleic acid aptamers, whole cells, or biomimetic receptors, with a physicochemical transducer. Among these, aptamers have emerged as powerful alternatives to antibodies due to their high stability, ease of synthesis, and adaptability for diverse targets, including small molecules and whole bacteria(Y. L. Tang, Li, Chen, Zhong, & Yang, 2025). Upon specific binding between the recognition element and the target analyte; the transducer converts this molecular interaction to a measurable signal (e.g.; electrical; optical; or mass-based); enabling quantitative detection (Turner, 2013).

Fiber-optic localized surface plasmon resonance (LSPR) sensors combine the advantages of optical fiber-optic platforms, such as compact size, low cost, portability, and immunity to electromagnetic interference, with the high refractive index sensitivity of plasmonic nanostructures, enabling on-site, real-time detection (Lei et al., 2023; Li et al., 2024; Zhang, Lei, Li, Wang, & Yan, 2024). These sensors have demonstrated remarkable performance in detecting large biomolecules; for example, Ning et al. (Ning et al., 2023) reported a fiber-optic LSPR sensor for circulating cell-free DNA with a low limit of detection (LOD) of 14.0 pM; while Xu et al. (B. Xu, Li, Xiang, Luo, & Huang, 2025) achieved a LOD of 1 pM for the SARS-CoV-2 nucleocapsid gene using gold nanorod-functionalized fiber-optic LSPR sensor. However; achieving comparable sensitivity for small-molecule targets remains challenging due to their minimal refractive index perturbation. Recent advances in nanomaterials; such as twisted bilayer graphene superlattices for optoelectronic biosensing; have pushed the boundaries of detection limits for biomolecular interactions(Du et al., 2025), highlighting the critical importance of nanomaterial engineering in enhancing sensor performance. Yet, these advanced materials often require complex fabrication and lack the portability needed for field deployment.

Detecting small-molecule analytes such as tetracycline remains challenging due to their minimal perturbation of the local refractive index. While other highly sensitive optical biosensing platforms, such as surface-enhanced Raman spectroscopy (SERS), have demonstrated exceptional performance in detecting low-abundance biomarkers(Ma et al., 2020); these approaches often involve intricate substrate fabrication; require sophisticated instrumentation; and are less amenable to rapid; on-site deployment. In contrast; fiber-optic LSPR biosensors offer a compelling alternative by combining portability; real-time capability; and ease of integration into field-deployable systems. A key limitation is the low surface density of plasmonic nanostructures that can be effectively immobilized on the fiber-optic sensing region; which constrains the LSPR signal shift upon analyte binding. This issue is particularly relevant in food safety: tetracycline residues in milk frequently exceed regulatory limits; and even low-dose; long-term exposure may pose health risks. Consequently; the EU and U.S. FDA have set strict maximum residue limits (MRLs) for tetracycline in milk (0.1 mg/kg and 0.3 mg/kg; respectively) (Liu, Zhang, et al., 2018; Meng et al., 2026; Wen et al., 2025). While conventional instrumental methods offer sufficient accuracy, they are ill-suited for on-site rapid screening, often delaying timely risk intervention. Therefore, enhancing the loading efficiency and spatial organization of nanosensing materials on optical fibers represents not only a critical research priority for boosting the sensitivity of fiber-optic LSPR biosensors in trace small-molecule detection (De Acha, Socorro-Leranoz, Elosúa, & Matías, 2021; Jiang, Huang, Liu, Shu, & Li, 2024), but also a pivotal step toward enabling rapid, on-site monitoring of tetracycline in milk and other high-risk foods—laying the groundwork for real-world food safety applications.

To address this challenge, this study proposed a fiber-optic aptamer sensor based on a DNA triple-helix molecular switch (THMS). THMS is formed when the third strand of DNA interacts with the purine-pyrimidine pairs through Hoogsteen hydrogen bonding and binds within the major groove of the double helix. This third strand is typically a triplex-forming oligonucleotide, which is rich in pyrimidine or purine (S. Tang et al., 2025). As shown in Scheme 1a; the THMS system consisted of a target-specific aptamer sequence with two arm segments and an oligonucleotide serving as a signal transduction probe (STP) (Verdian-Doghaei, Housaindokht, & Abnous, 2014). This triple-helix architecture offered higher sensitivity and enhanced stability than double-stranded DNA switches or molecular beacons; while preserving the original aptamer's selectivity and binding affinity. (Zheng et al., 2011). While THMS have been explored in electrochemical(Taghdisi et al., 2015) or fluorescence assays(T. X. Chen et al., 2017), their integration with fiber-optic LSPR transduction for active displacement-based signal amplification has not been reported. To our knowledge, this is the first application of THMS driven fiber LSPR sensors.

An 8-bp truncated single-stranded DNA (ssDNA) with high affinity for tetracycline was selected as the target-specific aptamer sequence to assemble the THMS with the signal transduction probe. The 8-bp ssDNA aptamer retains only the original stacking pocket and six additional specific bases, while exhibiting higher binding affinity (Kd of 1.067 nM for tetracycline)(Kwon, Raston, & Gu, 2014).As shown in Scheme 1b, the fiber-optic end face was hydroxylated using piranha solution and then treated with 3-aminopropyltriethoxysilane to introduce abundant amino (–NH_2) groups onto the fiber-optic surface and gold nanoparticles (AuNPs) were attached to the fiber-optic end face. The thiol-modified STP was incubated with the fiber-optic end face, allowing it to anchor onto the AuNPs immobilized on the fiber end face via Au—S bonds. Subsequently, a DNA triple-helix molecular switch was formed by incubating the functionalized fiber with a tetracycline aptamer (conjugated to AuNPs) that contained two complementary arm segments. In this configuration, plasmonic coupling between adjacent AuNPs induced a large red shift in the localized surface plasmon resonance (LSPR) absorption peak.

When target tetracycline was present, the aptamer exhibited a higher binding affinity for tetracycline than for the complementary strands in the DNA triple-helix molecular switch. Consequently, the triple-helix structure was disassembled, releasing the AuNPs serving as the signal tag from the fiber-optic end face. The loss of plasmonic coupling between the AuNPs resulted in a blue shift of the LSPR absorption peak. By monitoring this spectral shift, highly sensitive quantification of tetracycline was achieved.

2. Materials and methods

2.1. Materials

Sodium citrate tribasic, acetonitrile, sodium chloride, hydrogen peroxide (H_2O_2), glucose, bovine serum albumin (BSA), and maleic anhydride were purchased from National Pharmaceutical Group Chemical Reagents Co., Ltd. Chloroauric acid trihydrate ($HAuCl_4{\cdot}3H_2O$), 3-aminopropyltriethoxysilane (APTES), tetracycline, erythromycin, tobramycin, and oxytetracycline were supplied from Shanghai Aladdin Bio-Chem Technology Co., Ltd. The nucleic acid probes—signal transduction probe (STP): 5′-HS-$(CH_2)_6$-GAGAGAGAGAGAGA, and tetracycline aptamer: 5′-HS-$(CH_2)_6$-CTCTCTCGGTGGTGTCTCTC—were both synthesized by Sangon Biotech (Shanghai) Co., Ltd.

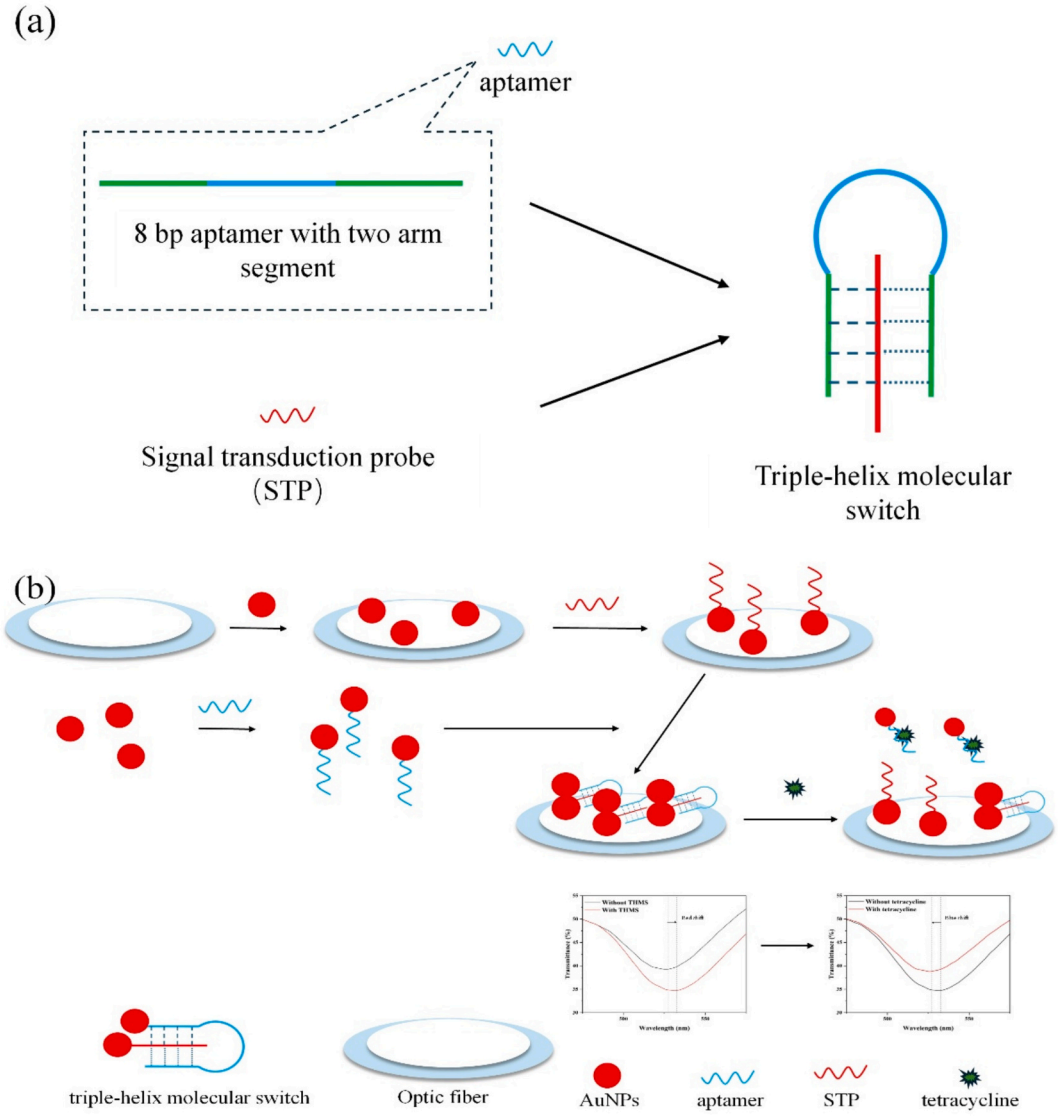

Scheme 1. Schematic illustration of the triple-helix molecular switch (THMS)-based fiber-optic LSPR aptasensor for tetracycline detection. (a) Architecture of the DNA triple-helix molecular switch. (b) Sensor fabrication and detection mechanism.

2.2. Methods

2.2.1. Preparation of the AuNPs

The AuNPs were synthesized using the seed-mediated growth method (Frens, 1973). Briefly, 100 mL 0.01% (*w/v*) $HAuCl_4$ solution was added to a three-neck flask and heated to boiling. Subsequently, 3.0 mL of 1.0% (w/v) sodium citrate solution was rapidly injected dropwise to the boiling mixture, which was then refluxed for 15 min. The solution color changed from pale yellow to dark purple and finally to a bright ruby red. After cooling to room temperature, the colloidal solution was stored in sealed vials at 4 °C for future use.

2.2.2. Construction of the FO LSPR sensor

10.0 μL 10.0 μM thiol-modified tetracycline aptamer was added to 10.0 mL AuNP dispersion. The aptamer formed stable Au—S bonds with the AuNPs, yielding an AuNP–aptamer conjugate (AuNP–apt) dispersion.

The fiber-optic end face was immersed in piranha solution (7:3 *v/v* concentrated H_2SO_4 to 30% H_2O_2) to a depth of approximately 2 cm at 80 °C for 40 min. After thorough rinsing with ultrapure water and drying under a stream of nitrogen gas, the surface was successfully hydroxylated. Then, the hydroxylated fiber-optic end face was immersed in a 1.0% (*v*/v) APTES solution (APTES:ethanol:water = 1:1:98, v/v/v) and incubated at 25 °C for 12 h. During this period, APTES undergoes hydrolysis, and the hydrolysis products undergo dehydration and condensation to form silanol condensates. These condensates undergo dehydration and condensation with the hydroxyl groups on the fiber end face, and a layer of organic molecules with terminal amino groups ($-NH_2$) is attached to the fiber surface through strong Si-O-Si covalent bonds. At this point, the fiber end face transitions from being rich in hydroxyl groups (-OH) to being rich in amino groups. Then, immerse the fiber end face in the AuNP solution and incubate it at 25 °C for 5 h. The negatively charged gold nanoparticles on the surface bind to the positively charged amino groups on the fiber surface through electrostatic interaction.

The AuNP-modified fiber-optic was immersed in a 10.0 μM solution of the thiol-modified STP and incubated at 25 °C for 12 h. After oxidation of the thiol group, its lonepair electrons are shared with gold atoms, forming a coordination bond (Au—S) with a strength close to that of a covalent bond. The thiol-modified STP is attached to the surface of gold nanoparticles through the terminal sulfur atom in the form of a covalent bond. To block the excess amino groups on the fiber-optic end face, it was immersed in 10.0 mM maleic anhydride for 1 h. Finally, the fiber-optic end face was immersed in the AuNP–apt solution and incubated

for 1 h to assemble the DNA THMS.

2.2.3. Optimization of sensor preparation and detection conditions

To enhance detection performance, critical parameters—including tetracycline-binding aptamer concentration, solution pH, and hybridization time—were systematically optimized.

STP concentration. The STP-functionalized fiber-optic tip was immersed in STP solutions (5.0–25.0 μM, in 5.0 μM increments) for 12 h, followed by incubation in the AuNP–aptamer conjugate solution (10.0 μM) at 25 °C for 1 h. The LSPR peak shift was recorded to assess aptamer loading efficiency.

Hybridization time. The STP-modified tip was incubated in the AuNP–aptamer solution at 25 °C, and the LSPR response was monitored every 20 min over 120 min to determine the optimal binding duration.

Solution pH. The sensor was exposed to 50 ng/mL tetracycline solutions adjusted to pH values from 6.5 to 8.5, and the resulting LSPR shifts were measured to evaluate pH-dependent recognition efficiency.

Detection time. The fiber-optic sensor was immersed in a 50 ng/mL tetracycline solution and incubated at 25 °C for durations ranging from 0.5 to 3.0 h. The time-dependent LSPR shifts were recorded to determine the optimal detection time for maximal signal response.

2.2.4. Detection of actual samples

For the measurement, the LSPR sensor was immersed in a tetracycline-containing sample solution to allow the aptamer to bind tetracycline, and the signal was analyzed using the LSPR sensing system. To assess the analytical performance of the proposed method on real samples, commercially available milk products were purchased from a local supermarket. Prior to analysis, the samples were pretreated following the Chinese National Standard Method (GB/T 22990–2008). Additionally, recovery experiments were conducted by spiking three independent milk samples with tetracycline at three different concentration levels. High-performance liquid chromatography (HPLC) was employed as the reference method. The results obtained from the proposed method were statistically compared with those from HPLC to evaluate accuracy.

3. Results and discussion

3.1. Characterization of the AuNPs

The synthesized AuNPs were characterized for their optical and morphological properties. The UV–Vis absorption spectrum (Fig. 1a) showed a distinct plasmonic peak at approximate 520 nm, which was consistent with previous reports (Y. C. Xu, Xiong, & Yan, 2021). TEM (HT7800, Hitachi, Tokyo, Japan) imaging further revealed that the AuNPs were spherical in shape, with an average diameter of around 20 nm and exhibited good dispersity (Fig. 1b). These properties confirmed that the synthesized AuNPs were suitable for the construction of the proposed fiber-optic LSPR sensor.

3.2. Characterization of fiber-optic end face

The LSPR signal is primarily governed by the density of aptamer-conjugated AuNP tags bound to the AuNPs immobilized on the fiber-optic end face, which modulates the local refractive index and plasmonic coupling. To monitor the stepwise sensor fabrication and detection process, scanning electron microscopy (SEM; Quanta FEG 250, FEI, Waltham, MA, USA) was used to characterize the fiber-optic tip at four key stages: (i) bare fiber, (ii) after AuNP immobilization, (iii) following assembly of the triple-helix molecular switch (THMS)-based sensor, and (iv) post tetracycline exposure. The corresponding SEM images are shown in Fig. 2.

Fig. 2a shows the pristine fiber-optic end face, exhibiting a smooth and uniform surface. After AuNP immobilization (Fig. 2b), nanoparticles were sparsely yet uniformly distributed without noticeable aggregation, providing favorable conditions for LSPR signal generation. Following assembly of the triple-helix molecular switch (THMS)-based sensor (Fig. 2c), a significant increase in surface nanoparticle density was observed, confirming successful incorporation of the AuNP-labeled aptamer component. Finally, after exposure to tetracycline (Fig. 2d), a marked reduction in nanoparticle coverage was evident, consistent with the target-induced displacement mechanism of the sensor.

3.3. Optimization of fabrication conditions for the LSPR Fiber-optic sensor

The signal intensity of the fiber-optic LSPR sensor developed in this study was strongly dependent on the number of the AuNP pair formed between the aptamer-AuNP signal tag and the AuNP immobilized on the fiber-optic end face (FO-AuNPs). The blue shift observed in the spectrum after tetracycline binding is a direct result of the disruption of plasma coupling between adjacent AuNP. In the assembled THMS configuration, the adapter labeled with AuNP is brought into close proximity to the AuNP fixed on the fiber end face through hybridization of complementary DNA strands, resulting in an increase in the density of AuNP

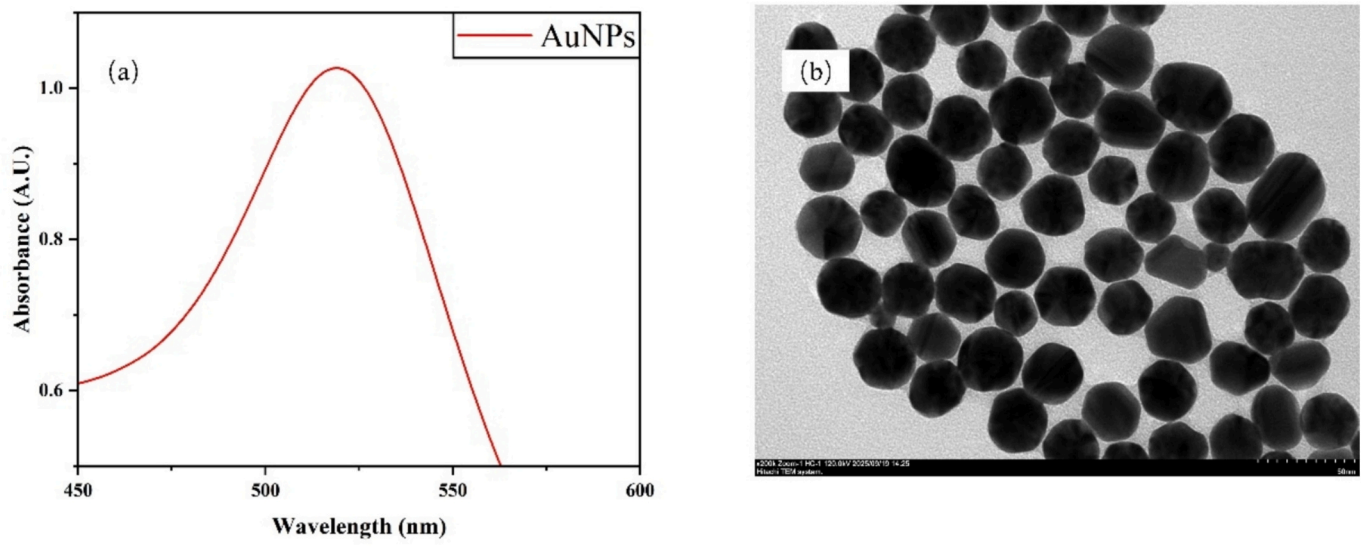

Fig. 1. Characterization of the AuNPs. (a) UV–Vis absorption spectrum. (b) TEM image.

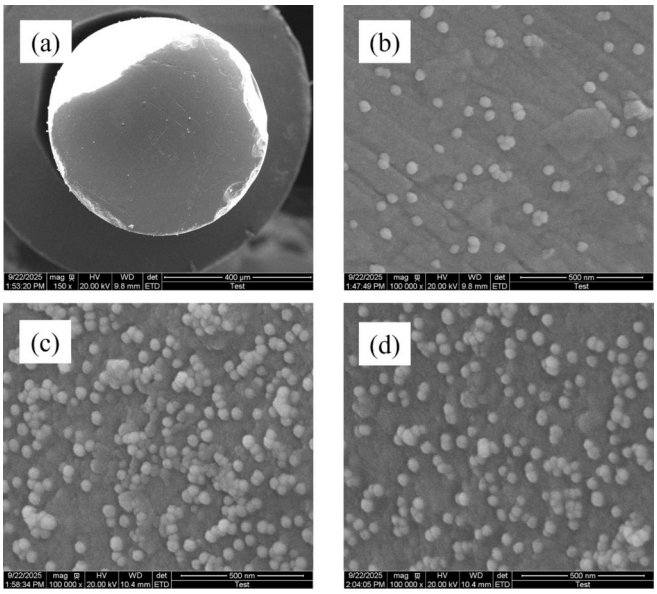

Fig. 2. SEM characterization of the fiber-optic end face at key fabrication and sensing stages. (a) Bare fiber. (b) After AuNP immobilization. (c) After assembly of the THMS. (d) After tetracycline exposure.

and a strong plasma coupling effect. The LSPR absorption peak undergoes a red shift. When tetracycline is present, the high affinity interaction between the adapter and the target analyte will outperform the stable triple helix structure of the hydrogen bond. This will trigger the dissociation of AuNPs adapter conjugates from the sensor surface, effectively increasing the average inter particle distance, reducing the density of AuNPs, and weakening the plasma coupling effect, manifested as a measurable blue shift in the absorption peak. Therefore, the STP concentration used in the functionalization of FO-AuNPs, the incubation time for binding between FO-AuNPs, and aptamer–AuNP signal tags were identified as a critical factor influencing sensor performance, and they were systematically optimized. The magnitude of the LSPR peak shift was used as the evaluation metric.

As shown in Fig. 3a, when the STP concentration was too low, an insufficient amount of STP was available to effectively mediate the binding between the aptamer–AuNP signal tags and the fiber-optic surface. Consequently, fewer nanoparticles were immobilized, leading to a diminished LSPR red shift. Conversely, at excessively high STP concentrations, the increased density of binding sites led to overcrowding of aptamer–AuNP signal tags on the fiber-optic surface. This induced steric hindrance and suboptimal interparticle spacing, which weakened plasmonic coupling and consequently yielded a small LSPR shift. Therefore, the maximum LSPR wavelength shift was obtained at an STP concentration of 20 μM.

The influence of the incubation time for aptamer–AuNP signal tag binding on sensor performance is shown in Fig. 3b. The LSPR wavelength shift increased progressively between 20 and 60 min and plateaued thereafter, with no significant further change observed beyond 60 min. Based on this saturation behavior, an incubation time of 60 min was selected as the optimal binding duration for the aptamer–AuNP signal tag.

To obtain optimal sensor performance, the pH of the working buffer played a critical role, as it directly influenced the conformation of the nucleic acid aptamer and the stability of the triple-helix structure. These structural changes, in turn, influenced the binding affinity between the tetracycline aptamer and tetracycline, thereby ultimately modulating the sensor's performance. The influence of pH on the sensor response was evaluated using 50 ng/mL tetracycline standard solutions buffered

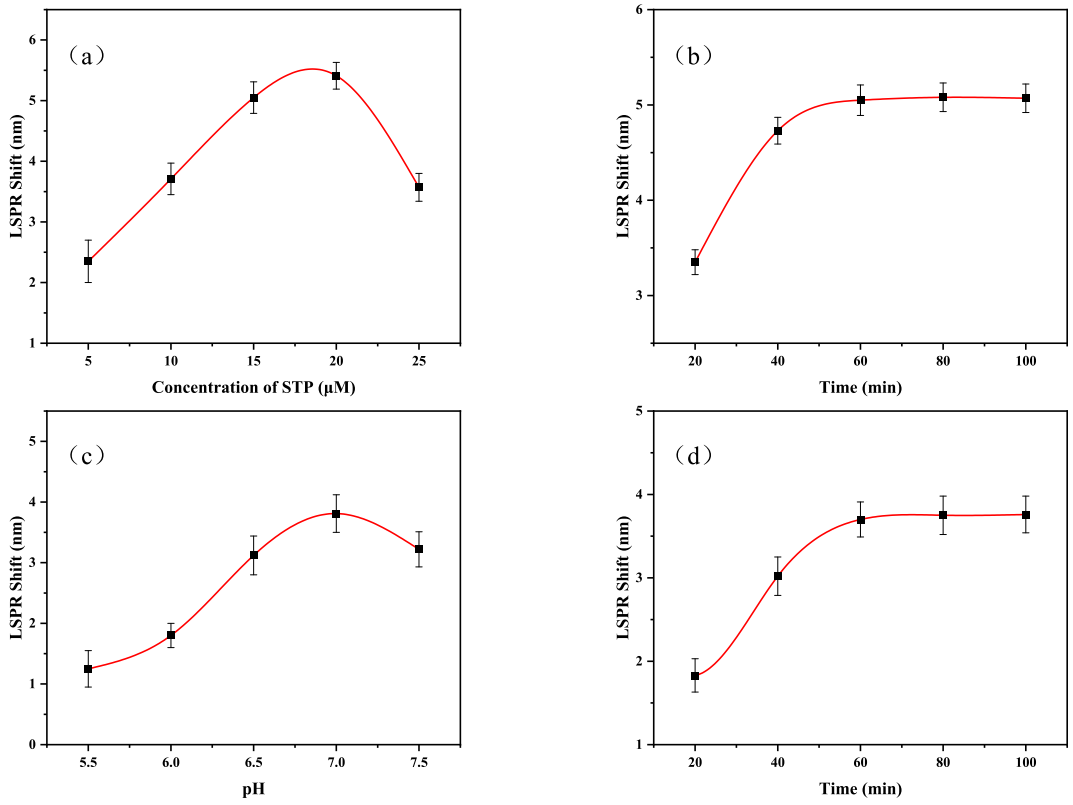

Fig. 3. Optimization of key fabrication and detection parameters for the LSPR fiber-optic sensor. (a) Effect of STP concentration on the LSPR response. (b) Effect of aptamer–AuNP hybridization time on sensor performance. (c) Effect of buffer pH on the LSPR response to 50 ng/mL tetracycline. (d) Effect of detection time on the LSPR response to tetracycline.

at pH values of 6.5, 7.0, 7.5, 8.0, and 8.5. As shown in Fig. 3c, the LSPR peak exhibited a blue shift that increased with rising pH up to 7.0, reaching a maximum magnitude at this point. Further increased in pH beyond 7.0 resulted in a gradual decrease in the blue shift. This trend suggested that pH 7.0 provided the most favorable environment for the conformational stability of the aptamer and the triple-helix structure, thereby maximizing the sensor response. Thus, pH 7.0 was selected as the optimal working pH for the detection system.

To determine the optimal detection time, the sensor response to a 50 ng/mL tetracycline standard solution was monitored, with the LSPR wavelength shift recorded at 20-min intervals over 20–100 min. As shown in Fig. 3d, the LSPR shift increased steadily from 20 to 60 min and then plateaued, showing no further significant change with prolonged incubation. Based on this saturation behavior, 60 min was selected as the optimal detection time for the sensor.

Notably, due to the relatively weak Hoogsteen hydrogen bonding, the triple-helix structure is thermally sensitive. For similar purine-motif triplexes, Pilch et al. reported a maximum melting temperature (Tm) of approximately 54 °C(Pilch, Levenson, & Shafer, 1991). Since all sensing experiments in this work were conducted at 25 °C—well below this threshold—the triple helix maintains its structural integrity during detection, ensuring a stable baseline and minimizing false positives caused by thermal dissociation. Although extreme ambient temperatures (>40 °C) could potentially compromise performance, such conditions are uncommon in typical on-site food safety screening scenarios.

3.4. Calibration curve and analytical performance of the LSPR fiber-optic sensor

The LSPR fiber-optic sensor was fabricated under the optimized conditions and evaluated for the quantitative detection of tetracycline. A series of tetracycline standard solutions with concentrations ranging from 5 to 100 ng/mL were analyzed to construct a calibration curve. Upon exposure to tetracycline, the free tetracycline molecule competitively bound to the aptamer with higher affinity than to the complementary strand within the triple-helix structure. This triggered the ligand AuNP signal tag to leave the sensor surface, reducing the local nanoparticle density and altering the refractive index in the vicinity of the plasmonic field. Consequently, the LSPR extinction peak exhibited a blue shift, the magnitude of which correlated with tetracycline concentration.

As shown in Fig. 4a, the normalized LSPR spectra showed a progressive blue shift with increasing tetracycline concentration. The shift increased steeply at low concentrations and gradually plateaued at higher levels (Fig. 4b), indicating saturation of the recognition sites. In the concentration range of 5–100 ng/mL, the blue shift showed a strong linear relationship with the logarithm of tetracycline concentration (Fig. 4c), yielding a calibration equation of $\Delta\lambda = a \log C + b$ and a coefficient of determination of $R^2 = 0.9845$. This defined the dynamic linear detection range of 5–100 ng/mL, and the limit of detection (LOD) was determined to be 0.28 ng/mL, calculated as 3σ/S from blank measurements ($n = 10$) and the slope of the calibration curve.

The detection performance of the proposed method was compared with previously reported approaches (Table 1). In terms of sensitivity, it achieved a lower LOD than most existing methods. Although some techniques offered a wider linear range, the dynamic range of this sensor fully covered the tetracycline concentration limits specified by the Chinese national standard for milk (GB/T 22990–2008). Moreover, the method featured simple operation and compatibility with a portable optical setup, making it well-suited for rapid, on-site screening of tetracycline residues in dairy products.

The developed sensor provides a favorable balance of sensitivity, speed, and practicality for on-site use. Its performance is competitive with other optical methods and approaches the operational ethos of advanced, lab-based plasmonic platforms designed for clinical nucleic acid detection(Z. Chen et al., 2022), but is repurposed here for the fielddeployable, on-site screening of small-molecule contaminants.

3.5. Selectivity, repeatability, and stability of the LSPR fiber-optic sensor

In real food samples, sensors may encounter interferences from various biomacromolecules and structurally similar antibiotics. To evaluate the selectivity of the developed sensor, standard solutions (100 ng/mL) of interferents of glucose (Glu), bovine serum albumin (BSA), erythromycin (ERY), tobramycin (TOB), and oxytetracycline (OXY) were detected alongside tetracycline and a blank control. As shown in Fig. 5, only tetracycline induced a significant LSPR blue shift, whereas all other tested substances produced responses comparable to the blank. These results demonstrated that the sensor had high selectivity toward tetracycline. Among tetracycline-class antibiotics, oxytetracycline is the closest structural analogue to tetracycline, differing only by a single hydroxyl group; thus, its negligible cross-reactivity supports the high specificity of the aptamer for tetracycline.

Repeatability and stability are critical parameters for evaluating sensor performance. To assess repeatability, five independently

Table 1
Analytical performance of the developed sensor in comparison with previously reported methods for tetracycline determination.

Methods	Detection Range (ng/mL)	LOD (ng/mL)
This work	5–100	0.28
fluorescence(J. Chen; Xu; Li; Xu; & Zhang; 2021)	666.65–31,110.10	408.9
HPLC - DAD(Liu et al.; 2018)	3000–80,000	770
electrochemical(Le; Pham; La; Phan; & Le; 2016)	10–3000 ng/mL	10

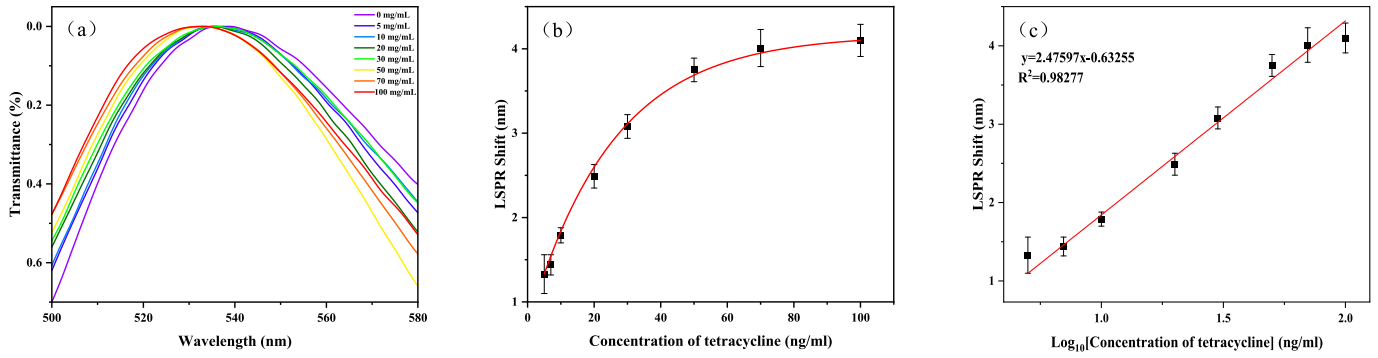

Fig. 4. LSPR response to varying tetracycline concentrations. (a) Normalized LSPR spectra at different tetracycline concentrations. (b) Nonlinear relationship between the LSPR peak shift and tetracycline concentration. (c) Linear correlation between the LSPR peak shift and the logarithm of tetracycline concentration.

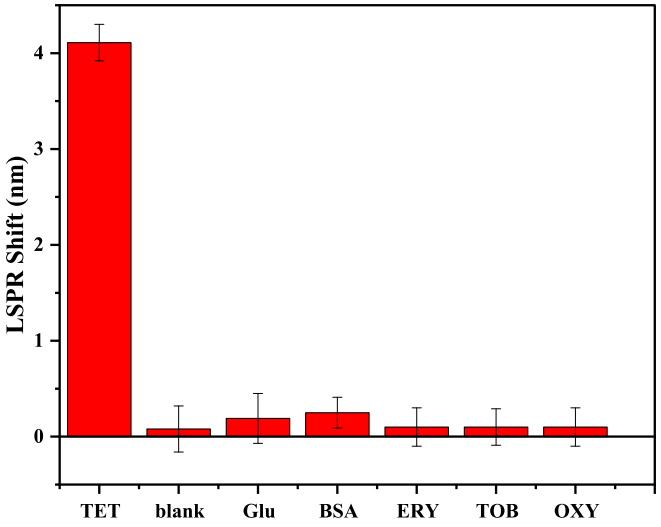

Fig. 5. Selectivity assessment of the sensor. LSPR response to tetracycline (100 ng/mL) compared with common interferents and blank.

fabricated LSPR fiber-optic sensors were used to detect a 50 ng/mL tetracycline standard solution under identical conditions. As shown in Fig. 6a, the LSPR peak shifts exhibited minimal variation, with a relative standard deviation (RSD) of 3.28%, indicating good inter-sensor repeatability. For long-term stability assessment, the sensors were stored at 4 °C and periodically tested over four weeks using a 50 ng/mL tetracycline solution. As shown in Fig. 6b, the LSPR response remained stable throughout the storage period, with a RSD of 1.41%, demonstrating excellent long-term stability. The fiber-optic LSPR sensor is designed for single-use operation in on-site screening scenarios to ensure reliability and avoid cross-contamination. Although the sensing surface can be regenerated in the laboratory by brief treatment with aqua regia—which effectively removes the gold nanoparticles and organic layers—this process involves hazardous chemicals and is not compatible with field deployment. Therefore, the sensor is intended to be used once per sample and then discarded, a practical approach for food safety applications where simplicity, speed, and contamination control are prioritized.

Collectively, these results confirmed that the developed LSPR fiber-optic sensor possessed both high repeatability and robust stability, making it suitable for practical applications.

3.6. Real-sample analysis

To evaluate the practical applicability of the LSPR sensor, milk was selected as the test matrix, and recovery experiments were conducted at three spiked tetracycline concentrations (20, 40, and 80 ng/mL). All samples were analyzed in triplicate using both the LSPR sensor and HPLC. As shown in Table 2, neither method detected tetracycline in the unspiked milk, confirming the absence of endogenous residues. Recoveries for the spiked samples ranged from 96.75% to 104.15%, with RSDs of 3.18–5.09%, indicating good accuracy and precision. A paired *t*-test yielded $p > 0.05$, demonstrating no statistically significant difference between the two methods. These results confirm that the LSPR sensor is reliable for the quantitative detection of tetracycline in real milk samples.

Although the detection process is supported by a novel fiber-optic LSPR sensing platform, its modular design and adaptability through molecular engineering also provide a feasible route for on-site monitoring of antibiotic residues in other food and environmental samples. Future work will focus on simultaneous detection of multiple antibiotics and the development of portable devices to meet broader needs in field-deployable food safety and environmental monitoring. Moreover, integrating such rapid detection platforms with emerging non-thermal intervention technologies—such as induced electric field treatments for microbial and spore inactivation in liquid foods(Xue et al., 2025) could enable a comprehensive “detect-totreat” strategy for ensuring the safety of thermally sensitive products like milk.

4. Conclusion

Aiming at the need for on-site monitoring of tetracycline residues in high-risk food milk, this study developed an innovative detection

Table 2
The detection result of tetracycline in milk by the method and the reference method.

Spiked (ng/mL)	HPLC (ng/mL)	This method (ng/mL)	Recovery (%)	RSD (%)[b]	*p*[c]
0	N.D.[a]	0.3 ± 0.07	–	–	–
20	20.91 ± 1.29	20.83 ± 1.06	104.15%	5.09%	0.26
40	38.56 ± 1.55	38.7 ± 1.77	96.75%	4.57%	0.10
80	77.59 ± 1.49	77.62 ± 2.47	97.03%	3.18%	0.70

[a] N.D.:Not detected.
[b] RSD:Relative standard deviation.
[c] p>0.05 Indicating no significant difference.

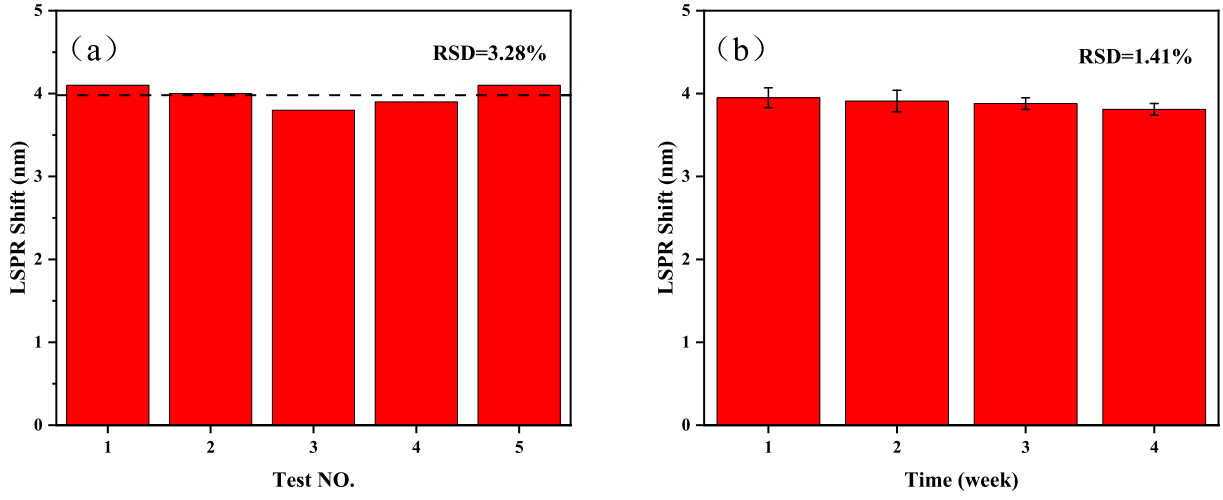

Fig. 6. Sensor performance: (a) Sensor repeatability (b) Sensor reproducibility.

method based on gold nanoparticle-labeled DNA triple-helix molecular switches. The approach utilizes a target-triggered disassembly process: tetracycline binding induces dissociation of a pre-assembled triple-helix structure immobilized on the fiber tip, leading to controlled release of AuNPs and a measurable LSPR blue-shift signal, thus enabling direct and rapid quantification.

Benefiting from the active shift amplification mechanism, the method showed excellent analytical performance in milk samples, with a linear detection range of 5–100 ng/mL, an ultra-low limit of detection of 0.28 ng/mL, high accuracy, and satisfactory recovery rates, demonstrating strong consistency with high-performance liquid chromatography results. Application to real milk samples confirmed its practical value for on-site food safety screening, allowing detection and prevention of health risks caused by tetracycline residue exceedance, especially in milk source supervision and distribution stages.

Although the detection process is supported by a novel fiber-optic LSPR sensing platform, its modular design and adaptability through molecular engineering also provide a feasible route for on-site monitoring of antibiotic residues in other food and environmental samples. Future work will focus on simultaneous detection of multiple antibiotics and the development of portable devices to meet broader needs in field-deployable food safety and environmental monitoring.

Furthermore, integrating advanced data analysis techniques, such as the machine learning models successfully applied to complex spectral data in clinical diagnostics(X. Y. Chen et al., 2024), could enhance the multiplexing capability and analytical robustness of our LSPR platform, enabling more intelligent and automated on-site screening.

CRediT authorship contribution statement

Xuqi Situ: Writing – original draft, Validation, Methodology, Investigation, Formal analysis. **Jiacong Li:** Validation, Investigation. **Yeshun Zhang:** Funding acquisition. **Hui Yan:** Writing – review & editing, Validation, Supervision, Methodology, Funding acquisition, Formal analysis, Conceptualization.

Fundings

This work was supported by the Key R&D Program of Zhenjiang (GJ2022008) and Earmarked Fund for Agriculture Research System of China (grant number: CARS-18).

Declaration of competing interest

The authors declare that they have no known competing financial interests or personal relationships that could have appeared to influence the work reported in this paper.

Data availability

Data will be made available on request.

References

Aga, D. S., Goldfish, R., & Kulshrestha, P. (2003). Application of ELISA in determining the fate of tetracyclines in land-applied livestock wastes. *Analyst, 128*(6), 658–662. https://doi.org/10.1039/b301630g

Angelette, A. L., Rando, L. L., Wadhwa, R. D., Barras, A. A., Delacroix, B. M., Talbot, N. C., … Kaye, A. D. (2023). Tetracycline-, doxycycline-, minocycline-induced pseudotumor cerebri and esophageal perforation. *Advances in Therapy, 40*(4), 1366–1378. https://doi.org/10.1007/s12325-023-02435-y

Chen, J., Xu, Y. L., Li, S. Y., Xu, F. H., & Zhang, Q. (2021). Ratio fluorescence detection of tetracycline by a Eu^{3+}/NH_2-MIL-53(Al) composite. *RSC Advances, 11*(4), 2397–2404. https://doi.org/10.1039/d0ra09185e

Chen, T. X., Ning, F., Liu, H. S., Wu, K. F., Li, W., & Ma, C. B. (2017). Label-free fluorescent strategy for sensitive detection of tetracycline based on triple-helix molecular switch and G-quadruplex. *Chinese Chemical Letters, 28*(7), 1380–1384. https://doi.org/10.1016/j.cclet.2017.01.006

Chen, X. Y., Chen, C., Tian, X. C., He, L., Zuo, E. G., Liu, P., … Lv, X. Y. (2024). DBAN: An improved dual branch attention network combined with serum Raman spectroscopy for diagnosis of diabetic kidney disease. *Talanta, 266*, 8. https://doi.org/10.1016/j.talanta.2023.125052

Chen, Z., Li, J. F., Li, T. Z., Fan, T. J., Meng, C. L., Li, C. Z., … Zhang, H. (2022). A CRISPR/Cas12a-empowered surface plasmon resonance platform for rapid and specific diagnosis of the omicron variant of SARS-CoV-2. *National Science Review, 9*(8), 10. https://doi.org/10.1093/nsr/nwac104

De Acha, N., Socorro-Leranoz, A. B., Elosúa, C., & Matías, I. R. (2021). Trends in the design of intensity-based optical fiber biosensors (2010−2020). *Biosensors-Basel, 11*(6), 197. https://doi.org/10.3390/bios11060197

Druzhinina, E. N. (1961). A microbiological method for separate determination of tetracycline and chlortetracycline in corresponding preparations. *Antibiotiki, 6*, 167–172. ://MEDLINE:13724512.

Du, B. W., Tian, X. L., Chen, Z., Ge, Y. Q., Chen, C. H., Gao, H. Y., … Zhang, H. (2025). Ultrasensitive optoelectronic biosensor arrays based on twisted bilayer graphene superlattice. *National Science Review, 12*(10), 10. https://doi.org/10.1093/nsr/nwaf357

Frens, G. (1973). Controlled nucleation for the regulation of the particle size in monodisperse gold suspensions. *Nature Physical Science, 241*(105), 20–22. https://doi.org/10.1038/physci241020a0

Gad, N. (2024). Development and validation of a multiresidue method for the determination of antibiotic residues in crawfish using LCMS/MS. *International Journal of Environmental Analytical Chemistry, 1-12*. https://doi.org/10.1080/03067319.2024.2384651

Jia, L., Zhang, Y. S., Zhu, T. F., & Xu, J. (2022). Study on visual multicolor intelligent detection of tetracycline antibiotics in various environmental samples by palygorskite-based fluorescent nano-probe. *Colloids and Surfaces A: Physicochemical and Engineering Aspects, 642*, Article 128690. https://doi.org/10.1016/j.colsurfa.2022.128690

Jiang, X. J., Huang, Q., Liu, H., Shu, X. W., & Li, C. L. (2024). Optical fiber biosensors based on surface plasmon resonance effect: A review. *IEEE Sensors Journal, 24*(19), 29506–29523. https://doi.org/10.1109/jsen.2024.3447283

Kwon, Y. S., Raston, N. H. A., & Gu, M. B. (2014). An ultra-sensitive colorimetric detection of tetracyclines using the shortest aptamer with highly enhanced affinity. *Chemical Communications, 50*(1), 40–42. https://doi.org/10.1039/c3cc47108j

Le, T. H., Pham, V. P., La, T. H., Phan, T. B., & Le, Q. H. (2016). Electrochemical aptasensor for detecting tetracycline in milk. *Advances in Natural Sciences: Nanoscience and Nanotechnology, 7*(1), Article 015008. https://doi.org/10.1088/2043-6262/7/1/015008

Lei, H., Zhu, S. H., Liu, C., Zhang, W., Chen, C., & Yan, H. (2023). Constructing the au nanoparticle multimer on optical fiber end face to enhance the signal of localized surface plasmon resonance biosensors: A case study for deoxynivalenol detection. *Sensors and Actuators B-Chemical, 380*, Article 133380. https://doi.org/10.1016/j.snb.2023.133380

Li, J. C., Ni, Y. X., Zhang, W., Nteppe, E. L. N., Li, Y. R., Zhang, Y. S., & Yan, H. (2024). Fiber optic LSPR sensing AFM1 in milk with enhanced sensitivity by the hot spot effect based on nanogap construction. *Micromachines, 15*(6), 779. https://doi.org/10.3390/mi15060779

Liu, D., Lu, L. L., Wang, M., Hussain, B., Tian, S. K., Luo, W. J., … Yang, X. E. (2019). Tetracycline uptake by pak choi grown on contaminated soils and its toxicity in human liver cell line HL-7702. *Environmental Pollution, 253*, 312–321. https://doi.org/10.1016/j.envpol.2019.06.086

Liu, F. Y., Zhang, X. F., Li, Y. Q., Gao, H., Ling, P. X., Li, X. Y., … Wang, F. S. (2018). Simultaneous screening and determination of eight tetracycline antibiotics illegally adulterated in herbal preparations using HPLC-DAD combined with LC-MS-MS. *Chromatographia, 81*(2), 303–314. https://doi.org/10.1007/s10337-017-3450-8

Liu, X. G., Huang, D. L., Lai, C., Zeng, G. M., Qin, L., Zhang, C., … Zhang, Y. J. (2018). Recent advances in sensors for tetracycline antibiotics and their applications. *TrAC Trends in Analytical Chemistry, 109*, 260–274. https://doi.org/10.1016/j.trac.2018.10.011

Ma, X. R., Cheng, H., Hou, J. W., Jia, Z. H., Wu, G. H., Lü, X. Y., … Chen, C. (2020). Detection of breast cancer based on novel porous silicon Bragg reflector surface-enhanced Raman spectroscopy-active structure. *Chinese Optics Letters, 18*(5), 5. https://doi.org/10.3788/col202018.051701

Madison, J. F. (1963). Tetracycline pigmentation of teeth. *Archives of Dermatology, 88*, 58–59. https://doi.org/10.1001/archderm.1963.01590190064008

Meng, Y., Sun, X., Xing, J., & Dong, C. (2026). Eu^{3+} doped carbon dots as a ratiometric fluorescence probe for highly sensitive detection of trace tetracycline in milk. *Spectrochimica Acta Part A: Molecular and Biomolecular Spectroscopy, 345*, Article 126811. https://doi.org/10.1016/j.saa.2025.126811

Ning, W., Zhang, C. Y., Tian, Z. Y., Wu, M. F., Luo, Z. W., Hu, S. M., … Li, Y. X. (2023). Ω-shaped fiber optic LSPR biosensor based on mismatched hybridization chain reaction and gold nanoparticles for detection of circulating cell-free DNA. *Biosensors & Bioelectronics, 228*, Article 115175. https://doi.org/10.1016/j.bios.2023.115175

Pilch, D. S., Levenson, C., & Shafer, R. H. (1991). Structure, stability, and thermodynamics of a short intermolecular purine-purine-pyrimidine triple helix. *Biochemistry, 30*(25), 6081–6088. https://doi.org/10.1021/bi00239a001

Pollard, A. T., & Morra, M. J. (2018). Fate of tetracycline antibiotics in dairy manure-amended soils. *Environmental Reviews, 26*(1), 102–112. https://doi.org/10.1139/er-2017-0041

Taghdisi, S. M., Danesh, N. M., Lavaee, P., Emrani, A. S., Ramezani, M., & Abnous, K. (2015). Aptamer biosensor for selective and rapid determination of insulin. *Analytical Letters, 48*(4), 672–681. https://doi.org/10.1080/00032719.2014.956216

Tang, S., He, B. S., Xie, L. L., Cao, X. Y., Ren, W. J., & Xu, Y. W. (2025). Exploring triplex DNA nanostructures: A comprehensive review from fundamentals to applications. *Chemical Engineering Journal, 505*, 17. https://doi.org/10.1016/j.cej.2025.159425

Tang, Y. L., Li, Y., Chen, P., Zhong, S., & Yang, Y. J. (2025). Nucleic acid aptamer-based sensors for Bacteria detection: A review. *Bioessays, 47*(3), 20. https://doi.org/10.1002/bies.202400111

Tsuji, K., & Goetz, J. F. (1978). HPLC as a rapid means of monitoring erythromycin and tetracycline fermentation processes. *Journal of Antibiotics, 31*(4), 302–308. https://doi.org/10.7164/antibiotics.31.302

Turner, A. P. F. (2013). Biosensors: sense and sensibility. *Chemical Society Reviews, 42*(8), 3184–3196. https://doi.org/10.1039/c3cs35528d

Verdian-Doghaei, A., Housaindokht, M. R., & Abnous, K. (2014). A fluorescent aptasensor for potassium ion detection-based triple-helix molecular switch. *Analytical Biochemistry, 466*, 72–75. https://doi.org/10.1016/j.ab.2014.08.014

Wang, X. R., Dong, Y. W., Luan, Y. X., Tian, S. N., Li, C., Li, Y., & Zhou, J. H. (2024). Integrated assessment of the spatial distribution, sources, degradation, and human risk of tetracyclines in honey in China. *Journal of Hazardous Materials, 473*, Article 134681. https://doi.org/10.1016/j.jhazmat.2024.134681

Wen, A. Y., Wang, H. H., Yuan, S. F., Yu, H., Guo, Y. H., & Yao, W. R. (2025). Underestimation of tetracycline antibiotic residues in chicken meat: The role of protein binding. *Food Chemistry, 463*, Article 141057. https://doi.org/10.1016/j.foodchem.2024.141057

Xu, B., Li, Y., Xiang, X. Y., Luo, Z. H., & Huang, J. L. (2025). Optical fiber LSPR sensor for SARS-CoV-2 N gene detection based on AuNRs. *Optics and Laser Technology, 180*, Article 111435. https://doi.org/10.1016/j.optlastec.2024.111435

Xu, Y. C., Xiong, M., & Yan, H. (2021). A portable optical fiber biosensor for the detection of zearalenone based on the localized surface plasmon resonance. *Sensors and Actuators B-Chemical, 336*, Article 129752. https://doi.org/10.1016/j.snb.2021.129752

Xue, L. P., Yang, N., Xu, X. M., Jin, Y. M., Cao, X. H., & Zhang, H. (2025). Inactivation of Geobacillus stearothermophilus spores by induced electric field in different food mediums. *Food Microbiology, 132*, 11. https://doi.org/10.1016/j.fm.2025.104832

Zhang, W., Lei, H., Li, J. C., Wang, X. Y., & Yan, H. (2024). Construction of the fiber optic LSPR sensor for highly sensitive detection of miR-103 by a dual signal enhancement strategy based on the hot-spot effect and HexSG4 catalysis. *Sensors and Actuators B-Chemical, 401*, Article 135004. https://doi.org/10.1016/j.snb.2023.135004

Zheng, J., Li, J. S., Jiang, Y., Jin, J. Y., Wang, K. M., Yang, R. H., & Tan, W. H. (2011). Design of aptamer-based sensing platform using triple-Helix molecular switch. *Analytical Chemistry, 83*(17), 6586–6592. https://doi.org/10.1021/ac201314y